# LANGMUIR

pubs.acs.org/Langmuir Article

# Simulation of Subnanometer Contrast in Dynamic Atomic Force Microscopy of Hydrophilic Alkanethiol Self-Assembled Monolayers in Water

Xiaoli Hu, Quanpeng Yang, Tao Ye, and Ashlie Martini\*



Cite This: Langmuir 2020, 36, 2240-2246



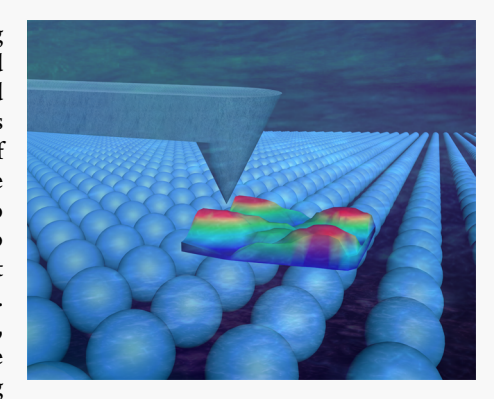
**Read Online** 

**ACCESS** 

III Metrics & More

Article Recommendations

ABSTRACT: Atomic resolution imaging of surfaces in liquid environments using atomic force microscopy (AFM) is challenging in terms of both reproducibility and measurement interpretation. To understand the origins of these challenges, we used molecular dynamics simulations of AFM on hydrophilic self-assembled monolayers (SAMs) in water. The force on the model AFM tip was calculated as a function of lateral and vertical position relative to the SAM surface. The contributions of the water and SAMs to the overall force were analyzed, and the former was correlated to the water density distribution. Then, dynamic AFM was modeled by oscillating the tip at a driving amplitude. It was found that the contrast between amplitudes at different lateral positions on the surface was dependent on the vertical position of the tip. Lastly, amplitude maps were produced for two vertical positions at constant height, and the ability to capture atomic resolution was related to the force on the tip. These results offer an explanation for the observed instability in atomic scale imaging using



AFM and more generally provide insight into the contrast mechanisms of surface images obtained in liquid environments.

### ■ INTRODUCTION

Dynamic atomic force microscopy (AFM) has been widely used to image various surfaces, including both organic and inorganic samples. 1-6 It has been shown that dynamic AFM can achieve higher spatial resolution than contact mode AFM by minimizing the interaction forces between the AFM tip and sample. 1,2,7 Such studies performed in vacuum environments routinely demonstrate the ability to image with atomic/molecular resolution. 8-10 There has also been significant interest in using AFM to study liquid-solid interfacial phenomena that are important to a wide range of technological applications, including electrocatalysis, biosensors, biomolecular adsorption, as well as lubrication and corrosion in tribology. 4,7 However, high-resolution AFM imaging in liquid is more challenging than in vacuum for several reasons. First, the oscillatory force due to solvation layers formed at the solid-liquid interfaces may affect the force sensitivity that is required for atomic resolution imaging. 11 In addition, in a liquid environment, the cantilever resonance has a low-quality factor, which leads to noise in force detection and degrades image resolution. Despite these challenges, recent studies have shown that atomic/molecular resolution can be obtained with dynamic AFM in liquid. 6,11-14 However, the stability and reproducibility of these measurements remain significant limitations. 15 Further, the interpretation of images obtained in liquid environments is challenging since the origin of the atomic scale contrast involves contributions from both the

surface being imaged and the liquid itself. For example, it has been suggested that atomic scale contrast observed in water originates from water molecules bound to the surface functional groups. This means that image contrast is due primarily to tip—water interactions, as opposed to the tip—sample interactions, which complicates the interpretation of images obtained in liquid environments.

Atomic resolution is directly related to the amplitude—distance or frequency shift—distance relationship measured during dynamic AFM, and these relationships are determined by the force acting on the tip. However, the interaction force is not directly observable in dynamic AFM experiments. <sup>3,17,18</sup> Therefore, density functional theory (DFT) calculations and molecular dynamics (MD) simulations that enable the direct calculation of interaction forces have been used to study atomic contrast in dynamic AFM. For example, DFT has been used to calculate individual force contributions, including Pauli repulsion, van der Waals, and electrostatic forces, to identify the dominant interactions responsible for molecular structure imaging. <sup>10,19–21</sup> However, due to computational limitations of the DFT method, only a few atoms can be considered, <sup>22</sup> so the

Received: November 26, 2019 Revised: February 1, 2020 Published: February 11, 2020



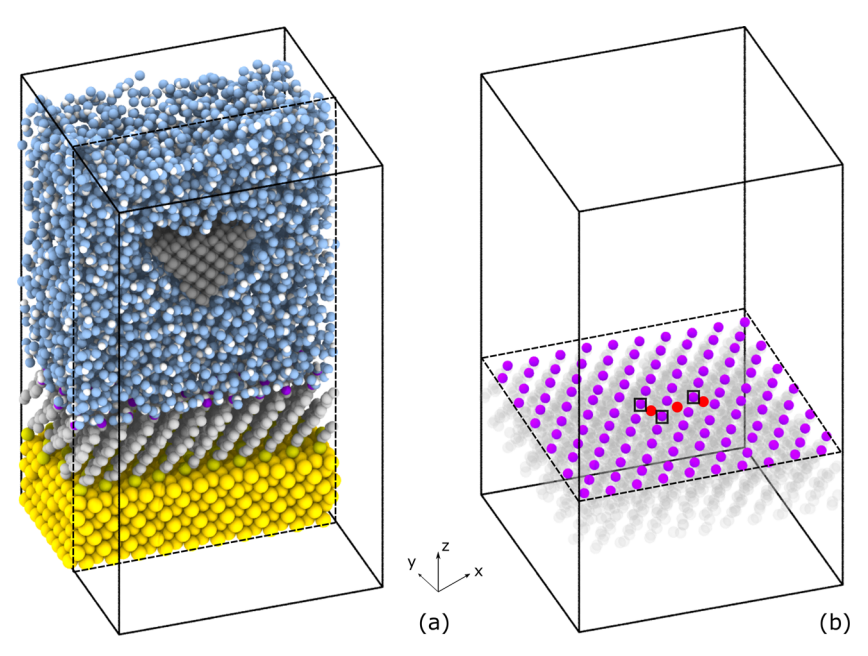


Figure 1. Perspective view snapshots of (a) half of the model system showing the conical tip and SAMs on Au(111) surface in water, and (b) terminal oxygen of the SAMs where the black squares and red circles represent the atom sites and hollow sites, respectively.

effects of larger-scale features, such as an elastic substrate or the tip beyond the few atoms at the apex, may not be captured. <sup>19</sup> The dynamic motion of an AFM tip has also not been modeled using DFT. Alternatively, MD simulations can describe more atoms and can capture dynamic processes. As such, MD simulations have been used to study atomic resolution in vacuum. <sup>23–25</sup> These studies used force—distance data from simulations of a static tip to calculate the frequency shift—distance relationship and then obtain surface images, but did not directly simulate the dynamic oscillation of the tip. Other studies have used MD to simulate dynamic AFM with tip oscillation, but did not report surface images or were not performed in a liquid environment. <sup>26–29</sup>

In this work, we performed MD simulations of dynamic AFM in liquid to understand the origins of atomic contrast. The model system consisted of an AFM tip apex and hydrophilic self-assembled monolayers (SAMs) in water. SAMs were chosen because they have well-defined structure and topography,<sup>30</sup> which facilitated the analysis of interaction forces in the model. Hydrophilic SAMs were then selected because the atomic resolution has been observed for hydrophilic surfaces in water experimentally. 12,14,31 The simulations were used to calculate the force that the tip experienced at different positions relative to the SAMs. Specifically, we analyzed forces at atom sites, corresponding to the lateral positions of the terminal oxygen atoms on the SAMs, and hollow sites, between the terminal oxygen atoms. The force on the tip at these two sites was analyzed in terms of the tip-SAM and tip-water interaction forces. The latter was correlated with the local distribution of water near the solid/ liquid interface. To obtain the amplitude-distance relationship, which determined the imaging contrast, the tip was oscillated over the atom and hollow sites and the amplitude was calculated. The amplitude-distance relationship was then analyzed in terms of the interaction force that the tip experienced at each site. Finally, amplitude maps from simulations of dynamic AFM at constant height illustrated that image contrast was highly dependent on the vertical

position of the tip relative to the surface being imaged. The results provided insight into the origin of the atomic contrast obtained using dynamic AFM in liquid.

#### METHODS

As shown in Figure 1a, the MD model consisted of a cone-shaped, diamond AFM tip apex and hydrophilic -S(CH<sub>2</sub>)<sub>11</sub>OH SAMs placed on an atomically flat Au(111) surface. The height of the tip was 1.2 nm, and the radius of the tip base was 0.9 nm. This tip geometry was motivated by the assumption that a few atoms protruding from the end of the tip are responsible for atomic scale contrast of dynamic AFM and that long-range interactions involving the rest of the tip are less important.  $^{19}$  The dimensions of the gold substrate were 5.0 nm  $\times$ 5.2 nm in the x and y directions, respectively. The sulfur head groups of the  $-S(CH_2)_{11}OH$  formed a  $(\sqrt{3} \times \sqrt{3})R30^\circ$  structure on the gold surface. The density of the SAMs was 0.216 nm<sup>2</sup> per chain, consistent with previous experiments and simulations.<sup>32–34</sup> The space between the top of the SAMs and the top of the simulation box ( $\Delta z =$ 6 nm) was filled with water. After relaxation, the average density of the water far from the SAM surface was 1.0 g/cm<sup>3</sup>. Simulations were run with the tip positioned in the water above three different atom sites and three different hollow sites, as illustrated in Figure 1b. These repeat simulations were run to capture the statistical fluctuations inherent to MD simulations. Periodic boundary conditions were applied in all directions.

The tip was treated as the rigid body, and the bottom 0.1 nm of the Au substrate was fixed. The lateral positions of the hydroxyl groups in the SAM molecules were fixed to ensure that the tip was located over the position of interest. This approach was consistent with a previous observation that the dominant response of SAMs to indentation was to deflect downwards as opposed to being pushed to the side. The interactions within the gold substrate were modeled by the embedded atom method (EAM). The water was described by extended simple point charge potential SPC/E. The united atom model was used to model the SAM molecules, where the hydrogen atoms were treated implicitly with their masses added to the corresponding carbon atom. Parameters for the interactions within the SAM molecules and between SAM molecules can be found in ref 38. For the O and H atoms in the hydroxyl group of SAM molecules, the partial charges and potential parameters were taken from ref 39. The thiol—Au interaction was modeled using a Morse potential. The Lennard-Jones potential and the Lorentz—Berthelot mixing rules were used

for all other long-range interactions. The same models and parameters for interatomic interactions in the system were used in our previous study of amplitude modulation (AM)-AFM of SAMs in water, where the only difference from the present study was the shape of the tip.<sup>27</sup> A Nosé-Hoover thermostat was applied to all nonconstrained atoms.

First, the system was equilibrated. This process included running the simulation in the NVT ensemble at 300 K for 50 ps to achieve steady-state potential energy, in the NPT ensemble for 50 ps at 300 K and 100 kPa to achieve steady-state volume and water density, and finally in the NVT ensemble at 300 K for 50 ps to again achieve steady-state potential energy. To calculate interaction forces, we equilibrated the system for another 250 ps in the NVT ensemble and calculated the average of the z-component of the total force, the force from the SAMs, and the force from the water acting on the tip as functions of the distance from the SAM surface. Distance d was defined as the vertical distance between the lowest atom in the tip and the average vertical position of oxygen atoms in the SAM molecules when the tip was far from the SAM surface.

The dynamic motion of the tip needed to model amplitude modulation (AM)-AFM was simulated using an approach we developed previously.<sup>29</sup> The tip was connected to a virtual atom through a harmonic spring with a stiffness of 40 N/m in the zdirection and then the virtual atom was moved with a sinusoidal motion perpendicular to the surface with a 0.1 nm amplitude and a frequency of 111 GHz. Small amplitude was applied here since it had been suggested that a small oscillation amplitude in dynamic AFM can enhance short-range interaction force sensitivity and thus lead to a higher spatial resolution.<sup>11</sup> The GHz scale of the frequency was necessitated by the small time scale of the simulation, but we have previously shown that trends in amplitude-distance data obtained from simulations with this frequency were consistent with those measured at the kHz scale in dynamic AFM experiments.<sup>27</sup> specific frequency used was chosen to maximize the amplitude<sup>5</sup> within the range available to the simulations. The ensemble of the tip and virtual atom was placed at different vertical positions to obtain the relationship between the tip's oscillation amplitude and its vertical distance from the SAM surface at the atom and hollow sites. All simulations were run with a time step of 0.25 fs using large-scale atomic/molecular massively parallel simulator (LAMMPS) software.4

# ■ RESULTS AND DISCUSSION

We first analyzed the total force acting on the tip as a function of distance from the SAM surface for the tip at the atom and hollow sites. The results are shown in Figure 2. When the tip is far from the surface, the total force acting on the tip is negligible at both the atom and hollow sites. Also, when the tip is indenting the SAMs (d = 0 corresponds to the plane of oxygen atoms that forms the surface of the SAMs), there is a large repulsive (positive) force at both sites. At intermediate distances, between 0 and 0.5 nm, the force oscillates between positive (repulsive) and negative (attractive). Force oscillation has been observed in previous measurements on mica and calcite surfaces immersed in water using dynamic AFM, where the force was calculated from the measured frequency shift.31,44 Importantly, comparing the force at the atom and hollow sites in our simulation results, the oscillations at intermediate distances exhibit opposite trends.

To understand the force trends described above, we analyzed the individual contributions of the water and the SAMs to the total force experienced by the tip. The force distribution at the atom site is shown in Figure 3a. At this site, when the tip is above the SAMs (d > 0.1 nm), a repulsive tip—water interaction is the major contribution to the total force. Then, there is a small attractive force from the tip—SAM interactions around d = 0.05 nm. Finally, a repulsive tip—SAM force becomes dominant after the tip begins to indent the

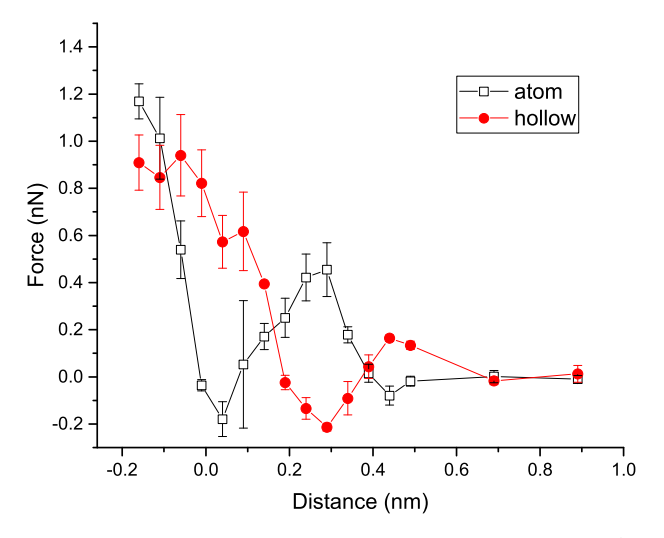


**Figure 2.** Total force on the tip at the atom sites and hollow sites (see Figure 1b) as a function of distance to the SAM surface. Error bars reflect the variation in force obtained at three different sites.

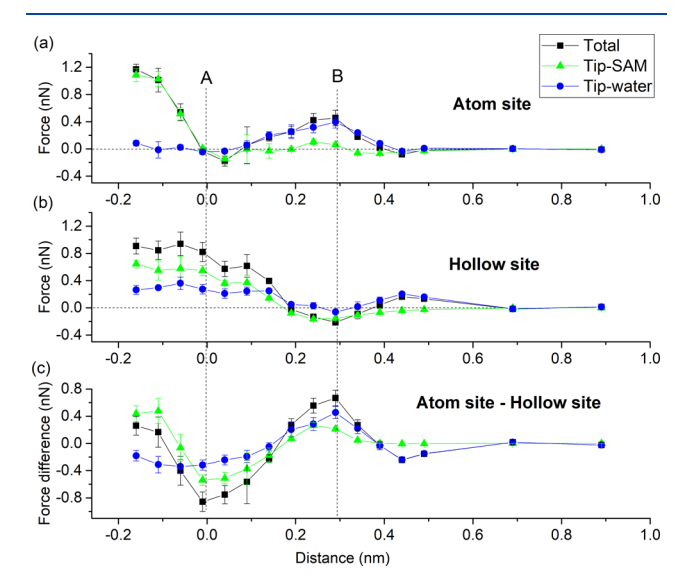


**Figure 3.** Force on the tip at the (a) atom and (b) hollow sites broken down into the tip—water and tip—SAM contributions. (c) Difference between the force at the atom and hollow sites. Distances at which the force difference is most significant are labeled A and B.

surface (d < 0). At hollow sites, as shown in Figure 3b, some trends are similar to those observed at the atom sites: there is a repulsive tip—water force when the tip is above the SAMs, a small attractive tip—SAM force as the tip is near the SAMs, and a large repulsive tip—SAM force when the tip indents the SAMs. However, there are differences between the trends as well. After indentation, the repulsive force between the tip and SAMs is smaller and the tip—water force is larger at the hollow sites compared to that at the atom sites. Also, and most significantly, the transitions from attractive to repulsive force occur further from the SAM surface at the hollow sites than at the atom sites.

The difference between the force at the atom and hollow sites, which is key to understanding the imaging contrast, was directly calculated by subtracting the force at the hollow sites (Figure 3b) from the force at the atom sites (Figure 3a), as shown in Figure 3c. The force difference is largest at two vertical positions, labeled A and B in Figure 3. When the tip is

at the SAM surface, at point A, the observed force difference is due predominantly to the repulsive tip—SAM and tip—water forces observed at the hollow site. Then, at point B, there is a force difference attributable to both the tip—SAM and tip—water interactions, where approximately one-third of the force difference is due to the attractive tip—SAM interactions at the hollow site, while the remaining two-thirds of the difference results from repulsive tip—water interactions at the atom site.

The difference in the tip—SAM forces may be attributed to the fact that the molecules in the SAM move away from the tip when it approaches the surface at the atom site, so the onset of the repulsive force occurs at a lower vertical position. In general, the largest differences between the atom and hollow sites are attributable to the tip—water forces, and we investigated the physical origins of these differences next.

The significant contribution of the tip—water forces shown above is consistent with the observations from a previous dynamic AFM study, which suggested that atomic scale contrast observed in the water originates from water molecules bound to the surface functional groups. <sup>16</sup> To understand the origin of the tip—water forces, we calculated the local density profile of the water above the hollow and atom sites on the surface as an average over 20 snapshots during a 200 ps duration. The results are reported in Figure 4a. As expected,

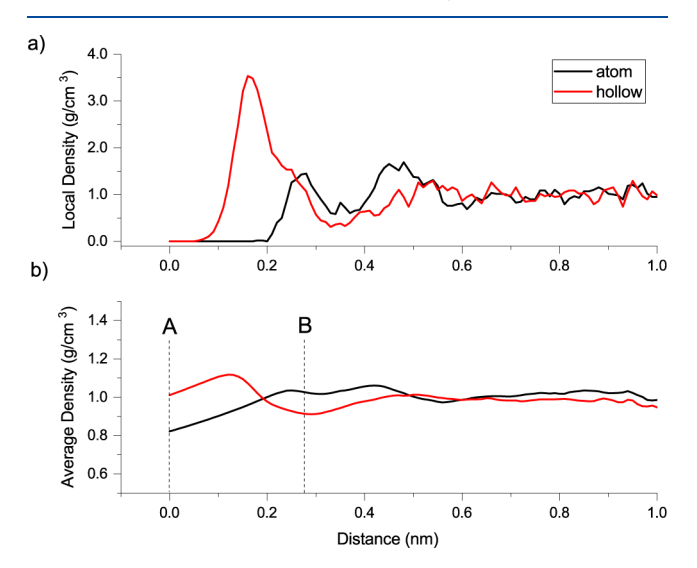


**Figure 4.** (a) Distribution of local water density as a function of distance from the SAM surface at the atom sites and hollow sites. Each point represents an average over cylindrical regions above 90 hollow and atom sites on the surface, and the standard deviation is approximately 0.27 g/cm<sup>3</sup> for each calculated average. (b) Water density across the tip obtained as an average of the local density over the region from the bottommost tip atom to the top of the tip.

the oscillation of the water density near the surface is observed due to the layering of the water molecules adjacent to the surface. The tip—water force originates from the interactions between the water and the entire body of the tip apex. For each vertical tip position, this is quantified as the average water density calculated from the position of the bottommost tip atom to the top of the tip, as shown in Figure 4b. At point A, the average water density across the tip is much higher at the hollow site, corresponding to the larger tip—water force at the hollow site in Figure 3b. At point B, the repulsive tip—water force at the atom site in Figure 3a can be correlated to the higher average water density across the tip in Figure 4b.

The force difference analysis above showed that both the tip—SAM and tip—water interactions contribute to the forces acting on the tip, which implies that both will affect image contrast. However, when the tip is further from the surface (e.g., at position B), the force difference is mainly due to the tip—water interactions at the atom sites. This suggests that the tip—water interaction is the dominant interaction responsible for atomic imaging in this case. However, when the tip is closer to the surface (e.g., at A), both the tip—water interaction and tip—SAM interaction contribute to the force difference acting on the tip between the atom sites and hollow sites. This indicates that the closer the tip comes to the surface, the more likely that the tip is imaging the surface rather than the water structure formed near the surface.

Next, the force difference calculated from simulations of a stationary tip is correlated to the amplitude measured from simulations of dynamic AFM. Amplitude is measured as a function of the distance from the SAM surface to the bottom of the tip at the center of its oscillation. The results are reported in Figure 5a. It can be seen that, at both sites, the

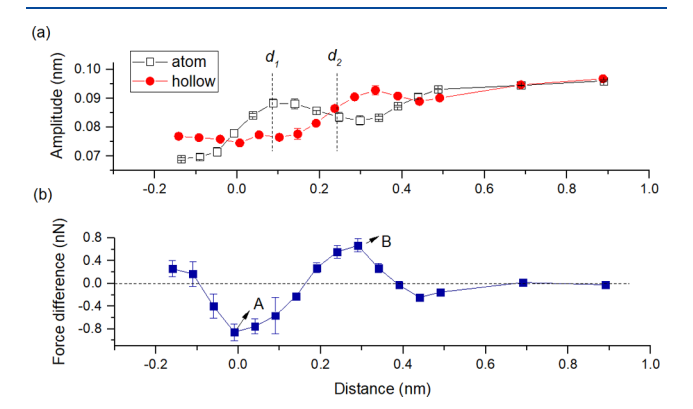


**Figure 5.** (a) Amplitude of tip oscillation from simulations of dynamic AFM and (b) force difference between the atom and hollow sites from static simulations as functions of the tip—SAM distance. In (a),  $d_1$  and  $d_2$  identify the distances where the amplitude differences between the atom and hollow sites are large and small, respectively.

amplitude increases with the distance between the tip and SAMs until it approaches a constant value, i.e., the free amplitude. Also, the amplitude is observed to oscillate with increasing distance from the surface. This amplitude oscillation has been observed in previous simulations. Amplitude oscillation is observed at both hollow and atom sites, but the oscillations are out of phase with each other.

Previous work has shown that a smaller oscillation amplitude can be correlated to a larger force on the tip.<sup>2</sup> This is observed here in a comparison between the amplitude and force difference, which is re-plotted in Figure 5b. When the tip is far from the surface, the amplitudes at the atom and hollow sites are similar, corresponding to a negligible force difference. At point A, the force difference is negative and the amplitude is larger at the atom sites. Then at B, the force difference is positive, resulting in a larger amplitude at the hollow sites. Note that the positions of the maximum force differences are shifted slightly (~0.05 nm) relative to the positions of the largest difference in amplitude. This offset is due to the fact that the distance and force were calculated with a static model tip, while amplitude was obtained from simulations of an oscillating tip where just the equilibrium position was used to calculate the distance.

The above analysis suggests that greater contrast (and, in turn, higher resolution) should be achieved with dynamic AFM measurements performed at distances where the amplitude difference between sites on the surfaces is largest. To test this, we performed additional dynamic AFM simulations in constant height mode. These simulations were performed at d=0.09 nm, where the amplitude difference between the atom sites and hollow sites is largest, and at d=0.24 nm, where the amplitude difference is negligible; these two vertical positions are labeled  $d_1$  and  $d_2$  in Figure 5a. The tip was oscillated over 70 lateral positions on the surface, and the amplitude of tip oscillation was recorded. The resultant amplitude maps are shown in Figure 6. It can be seen that atomic resolution is

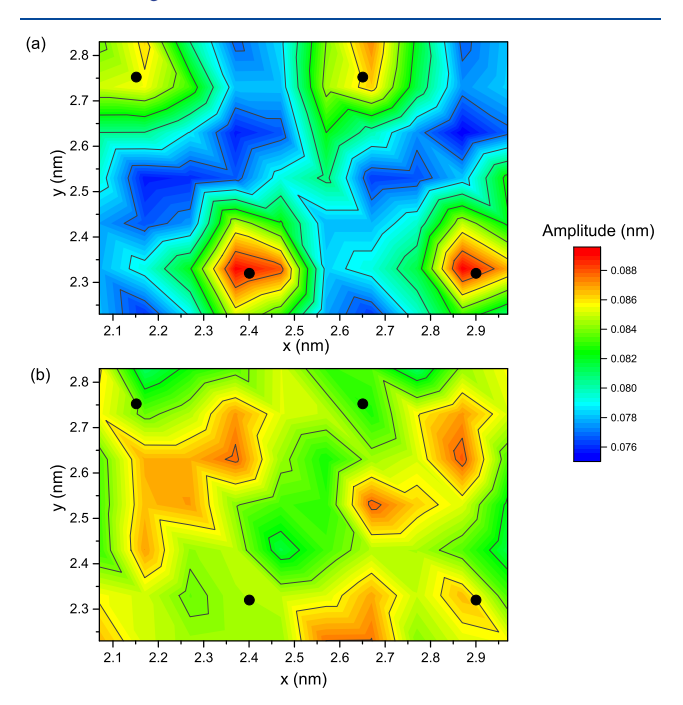


**Figure 6.** Simulated amplitude map at (a)  $d_1 = 0.09$  nm where force contrast between the atom and hollow sites is large and so the image resolution is high, and (b)  $d_2 = 0.24$  nm where the force difference is negligible and the image resolution is correspondingly poor. The black circles represent the positions of the SAMs terminal oxygen atoms.

observed at  $d_1$ , as evidenced by amplitude contrast that reflects the SAM lattice. The contrast is small ( $\sim$ 0.015 nm) but is statistically significant relative to the small driving amplitude of 0.1 nm. However, this contrast is not observed at  $d_2$ , indicating that atomic resolution could not be achieved at this height.

The simulation results clearly show that the ability to capture atomic resolution in such measurements is dependent on the vertical position of the tip. Although these results were obtained at constant height, they are directly relevant to dynamic AFM measurement performed at constant amplitude (AM-AFM). To determine the effect of amplitude on the resolution, Figure 5a can be analyzed in terms of the distance as a function of amplitude. For example, for an amplitude of 0.095 nm or larger, the height would be the same at both the atom and hollow sites, which indicates that atomic resolution would not be observed. Then, if the amplitude was set between 0.08 and 0.095 nm, there would be multiple heights corresponding to the target amplitude at either the atom or hollow sites. This may result in unstable imaging, which has

been observed in previous AM-AFM measurements. <sup>47</sup> However, for an amplitude between 0.075 and 0.08 nm, there is only one tip height at the atom sites and at the hollow sites, and the tip position at the hollow sites would be higher than that at the atom sites. This indicates that atomic resolution would be expected for an amplitude set in this range. Further, the resolution that is achieved would be due to both the tip—water and tip—SAM interactions.

#### CONCLUSIONS

Simulations were performed to investigate the mechanisms underlying atomic resolution images obtained using dynamic AFM in liquid. Simulations of a static AFM tip in the water near a hydrophilic SAM surface showed that the force on the tip is affected by both its vertical position and its lateral position relative to the SAM lattice. The variation in force was attributed to both the tip-SAM and tip-water interactions. Importantly, it was shown that the relative contributions of these two interactions to the total force depend on the distance from the SAM surface. This implies that image contrast is likely due to both the surface being imaged and the water, where the effect of the water will be larger when the tip is further from the surface. However, because the water density distribution is affected by the positions of atoms on the surface, both the tip water and tip-surface interactions can reflect the local surface structure.

Next, the simulation was extended to capture the oscillatory tip motion of a dynamic AFM measurement. The model tip amplitude increased with the distance from the surface approaching the free amplitude and also fluctuated with the distance to the surface, as observed in previous studies. 18, Here, we showed that these fluctuations depend not only on vertical position but also on the lateral position relative to the SAM lattice. The effect is that the amplitude of the oscillation of the tip at the atom and hollow sites is the same at some vertical positions and different at others. The effect of this observation on image contrast was demonstrated by simulating constant height amplitude maps of the surface with the tip at two different vertical positions. In one case, the amplitude was different at the atom and hollow sites, so the amplitude map reflected atomic resolution. However, in the other case, there was no amplitude contrast and so atomic resolution could not be achieved. This result suggests that the reproducibility of surface measurements using dynamic AFM is very sensitive to the vertical distance from the surface. This sensitivity is more severe in liquid environments (compared to vacuum) because of the contribution of the liquid to the amplitude fluctuations at different positions on the surface.

Overall, this study provides three important physical insights. First, the simulations show that image contrast is due to both the surface being imaged and water, with the effect of water being larger when the tip is further from the surface. This finding is expected to be relevant to imaging in any liquid environment. Second, the reproducibility of surface imaging using dynamic AFM is demonstrated to be sensitive to the vertical distance from the surface. Although this was observed only for different tip heights in the simulations, the results have a direct implication for other factors that affect vertical position, such as amplitude. Further, any parameter that affects the force on the tip, such as tip size and shape and the hydrophobicity of the tip and SAMs, can be expected to affect the ability to capture atomic resolution. Lastly, these simulations provide a means of directly correlating imaging

force to image resolution. Specifically, such simulations can predict the difference between the force on the tip at different lateral positions of interest on any model surface, which then could be correlated to anticipated contrast in amplitude (at constant height) or height (at constant amplitude or frequency).

Beyond these specific outcomes, the simulations reported here may stimulate future experimental studies into AFM contrast mechanisms. For example, three-dimensional AFM imaging, where amplitude—distance curves are acquired at each point in a scan area, <sup>4</sup> can provide direct information of the relationship between amplitude, height, and atomic scale imaging contrast. By combining experiments and atomistic simulations of imaging, we will begin to understand how atomic scale interactions between a tip apex, liquid, and sample lead to subnanometer scale contrast. Such insights can not only improve the reproducibility of imaging but also facilitate interpretation of the structures observed in atomic resolution images.

#### AUTHOR INFORMATION

# **Corresponding Author**

Ashlie Martini — Department of Mechanical Engineering, University of California-Merced, Merced, California 95343, United States; © orcid.org/0000-0003-2017-6081; Email: amartini@ucmerced.edu

#### **Authors**

Xiaoli Hu — Department of Mechanical Engineering, University of California-Merced, Merced, California 95343, United States Quanpeng Yang — Department of Mechanical Engineering, University of California-Merced, Merced, California 95343, United States

Tao Ye — Department of Chemistry and Chemical Biology, University of California-Merced, Merced, California 95343, United States

Complete contact information is available at: https://pubs.acs.org/10.1021/acs.langmuir.9b03655

#### Notes

The authors declare no competing financial interest.

# ACKNOWLEDGMENTS

This research was supported by the National Science Foundation through Grant #CHE 1808213 and the NASA Merced nAnomaterials Center for Energy and Sensing (MACES) through the support of the National Aeronautics and Space Administration (NASA) Grant no. NNX15AQ01.

# REFERENCES

- (1) Zhong, Q.; Inniss, D.; Kjoller, K.; Elings, V. Fractured polymer/silica fiber surface studied by tapping mode atomic force microscopy. *Surf. Sci. Lett.* **1993**, 290, L688–L692.
- (2) Jäggi, R. D.; Franco-Obregon, A.; Studerus, P.; Ensslin, K. Detailed analysis of forces influencing lateral resolution for Q-control and tapping mode. *Appl. Phys. Lett.* **2001**, *79*, 135–137.
- (3) Guzman, H. V.; Perrino, A. P.; Garcia, R. Peak forces in high-resolution imaging of soft matter in liquid. *ACS Nano* **2013**, *7*, 3198–3204.
- (4) Fukuma, T.; Garcia, R. Atomic-and molecular-resolution mapping of solid-liquid interfaces by 3D atomic force microscopy. *ACS Nano* **2018**, *12*, 11785–11797.
- (5) García, R.; Perez, R. Dynamic atomic force microscopy methods. *Surf. Sci. Rep.* **2002**, *47*, 197–301.

- (6) Voïtchovsky, K.; Kuna, J. J.; Contera, S. A.; Tosatti, E.; Stellacci, F. Direct mapping of the solid-liquid adhesion energy with subnanometre resolution. *Nat. Nanotechnol.* **2010**, *5*, 401–405.
- (7) Zaera, F. Probing liquid/solid interfaces at the molecular level. *Chem. Rev.* **2012**, *112*, 2920–2986.
- (8) Giessibl, F. J. Atomic resolution of the silicon (111)-(7x7) surface by atomic force microscopy. *Science* **1995**, 267, 68–71.
- (9) de Óteyza, D. G.; Gorman, P.; Chen, Y.-C.; Wickenburg, S.; Riss, A.; Mowbray, D. J.; Etkin, G.; Pedramrazi, Z.; Tsai, H.-Z.; Rubio, A.; Crommie, M. F.; et al. Direct imaging of covalent bond structure in single-molecule chemical reactions. *Science* **2013**, *340*, 1434–1437.
- (10) Gross, L.; Mohn, F.; Moll, N.; Schuler, B.; Criado, A.; Guitián, E.; Peña, D.; Gourdon, A.; Meyer, G. Bond-order discrimination by atomic force microscopy. *Science* **2012**, *337*, 1326–1329.
- (11) Fukuma, T. Subnanometer-resolution frequency modulation atomic force microscopy in liquid for biological applications. *Jpn. J. Appl. Phys.* **2009**, *48*, No. 08JA01.
- (12) Ebeling, D.; Solares, S. D. Amplitude modulation dynamic force microscopy imaging in liquids with atomic resolution: comparison of phase contrasts in single and dual mode operation. *Nanotechnology* **2013**, *24*, No. 135702.
- (13) Miller, E. J.; Trewby, W.; Payam, A. F.; Piantanida, L.; Cafolla, C.; Voïtchovsky, K. Sub-nanometer resolution imaging with amplitude-modulation atomic force microscopy in liquid. *J. Visualized Exp.* **2016**, No. e54924.
- (14) Fukuma, T.; Kobayashi, K.; Matsushige, K.; Yamada, H. True atomic resolution in liquid by frequency-modulation atomic force microscopy. *Appl. Phys. Lett.* **2005**, *87*, No. 034101.
- (15) Akrami, S.; Nakayachi, H.; Watanabe-Nakayama, T.; Asakawa, H.; Fukuma, T. Significant improvements in stability and reproducibility of atomic-scale atomic force microscopy in liquid. *Nanotechnology* **2014**, *25*, No. 455701.
- (16) Fukuma, T.; Higgins, M. J.; Jarvis, S. P. Direct imaging of lipidion network formation under physiological conditions by frequency modulation atomic force microscopy. *Phys. Rev. Lett.* **2007**, *98*, No. 106101.
- (17) Guzman, H. V.; Garcia, R. Peak forces and lateral resolution in amplitude modulation force microscopy in liquid. *Beilstein J. Nanotechnol.* **2013**, *4*, 852–859.
- (18) Hernández-Muñoz, J.; Chacón, E.; Tarazona, P. Density functional analysis of atomic force microscopy in a dense fluid. *J. Chem. Phys.* **2019**, *151*, No. 034701.
- (19) Gross, L.; Mohn, F.; Moll, N.; Liljeroth, P.; Meyer, G. The chemical structure of a molecule resolved by atomic force microscopy. *Science* **2009**, 325, 1110–1114.
- (20) Moll, N.; Gross, L.; Mohn, F.; Curioni, A.; Meyer, G. The mechanisms underlying the enhanced resolution of atomic force microscopy with functionalized tips. *New J. Phys.* **2010**, *12*, No. 125020.
- (21) Schneiderbauer, M.; Emmrich, M.; Weymouth, A. J.; Giessibl, F. J. CO tip functionalization inverts atomic force microscopy contrast via short-range electrostatic forces. *Phys. Rev. Lett.* **2014**, *112*, No. 166102.
- (22) Sanna, S.; Dues, C.; Schmidt, W. Modeling atomic force microscopy at LiNbO<sub>3</sub> surfaces from first-principles. *Comput. Mater. Sci.* **2015**, *103*, 145–150.
- (23) Abdurixit, A.; Baratoff, A.; Meyer, E. Molecular dynamics simulations of dynamic force microscopy: applications to the Si (111)-7× 7 surface. *Appl. Surf. Sci.* **2000**, *157*, 355–360.
- (24) Pishkenari, H. N.; Meghdari, A. Surface defects characterization with frequency and force modulation atomic force microscopy using molecular dynamics simulations. *Curr. Appl. Phys.* **2010**, *10*, 583–591.
- (25) Shiokawa, T.; Ohzono, T.; Fujihira, M. Molecular dynamics simulation of non-contact atomic force microscopy of an ordered monolayer consisting of single united atoms chemisorbed strongly on a continuum substrate. *Appl. Surf. Sci.* **2003**, 210, 117–122.
- (26) Xu, R.-G.; Leng, Y. Contact stiffness and damping of liquid films in dynamic atomic force microscope. *J. Chem. Phys.* **2016**, *144*, No. 154702.

- (27) Hu, X.; Nanney, W.; Umeda, K.; Ye, T.; Martini, A. Combined Experimental and Simulation Study of Amplitude Modulation Atomic Force Microscopy Measurements of Self-Assembled Monolayers in Water. *Langmuir* **2018**, 34, 9627–9633.
- (28) Hu, X.; Chan, N.; Martini, A.; Egberts, P. Tip convolution on HOPG surfaces measured in AM-AFM and interpreted using a combined experimental and simulation approach. *Nanotechnology* **2017**, 28, No. 025702.
- (29) Hu, X.; Egberts, P.; Dong, Y.; Martini, A. Molecular dynamics simulation of amplitude modulation atomic force microscopy. *Nanotechnology* **2015**, *26*, No. 235705.
- (30) Schwartz, D. K. Mechanisms and kinetics of self-assembled monolayer formation. *Annu. Rev. Phys. Chem.* **2001**, *52*, 107–137.
- (31) Fukuma, T.; Ueda, Y.; Yoshioka, S.; Asakawa, H. Atomic-scale distribution of water molecules at the mica-water interface visualized by three-dimensional scanning force microscopy. *Phys. Rev Lett.* **2010**, *104*, No. 016101.
- (32) Ghorai, P. K.; Glotzer, S. C. Molecular dynamics simulation study of self-assembled monolayers of alkanethiol surfactants on spherical gold nanoparticles. *J. Phys. Chem. C* **2007**, *111*, 15857–15862.
- (33) Hinterwirth, H.; Kappel, S.; Waitz, T.; Prohaska, T.; Lindner, W.; Lämmerhofer, M. Quantifying thiol ligand density of self-assembled monolayers on gold nanoparticles by inductively coupled plasma-mass spectrometry. ACS Nano 2013, 7, 1129–1136.
- (34) Majumdar, S.; Sierra-Suarez, J. A.; Schiffres, S. N.; Ong, W.-L.; Higgs, C. F., III; McGaughey, A. J.; Malen, J. A. Vibrational mismatch of metal leads controls thermal conductance of self-assembled monolayer junctions. *Nano Lett.* **2015**, *15*, 2985–2991.
- (35) Leng, Y.; Jiang, S. Atomic indentation and friction of self-assembled monolayers by hybrid molecular simulations. *J. Chem. Phys.* **2000**, *113*, 8800–8806.
- (36) Grochola, G.; Russo, S. P.; Snook, I. K. On fitting a gold embedded atom method potential using the force matching method. *J. Chem. Phys.* **2005**, *123*, No. 204719.
- (37) Berendsen, H.; Grigera, J.; Straatsma, T. The missing term in effective pair potentials. *J. Phys. Chem. A* **1987**, *91*, 6269–6271.
- (38) Ong, W.-L.; Majumdar, S.; Malen, J. A.; McGaughey, A. J. Coupling of organic and inorganic vibrational states and their thermal transport in nanocrystal arrays. *J. Phys. Chem. C* **2014**, *118*, 7288–7205
- (39) Hautman, J.; Bareman, J. P.; Mar, W.; Klein, M. L. Molecular dynamics investigations of self-assembled monolayers. *J. Chem. Soc., Faraday Trans.* **1991**, *87*, 2031–2037.
- (40) Mahaffy, R.; Bhatia, R.; Garrison, B. J. Diffusion of a butanethiolate molecule on a Au {111} surface. *J. Phys. Chem. B* **1997**, *101*, *771*–*773*.
- (41) Sung, I.-H.; Kim, D.-E. Molecular dynamics simulation study of the nano-wear characteristics of alkanethiol self-assembled monolayers. *Appl. Phys. A* **2005**, *81*, 109–114.
- (42) Allen, M. P.; Tildesley, D. J. Computer Simulation of Liquids; Oxford University Press, 2017.
- (43) Plimpton, S. Fast parallel algorithms for short-range molecular dynamics. *J. Comput. Phys.* **1995**, *117*, 1–19.
- (44) Fukuma, T.; Reischl, B.; Kobayashi, N.; Spijker, P.; Canova, F. F.; Miyazawa, K.; Foster, A. S. Mechanism of atomic force microscopy imaging of three-dimensional hydration structures at a solid-liquid interface. *Phys. Rev. B* **2015**, *92*, No. 155412.
- (45) Jensen, M. Ø.; Mouritsen, O. G.; Peters, G. H. The hydrophobic effect: Molecular dynamics simulations of water confined between extended hydrophobic and hydrophilic surfaces. *J. Chem. Phys.* **2004**, *120*, 9729–9744.
- (46) Pertsin, A.; Grunze, M. Water- graphite interaction and behavior of water near the graphite surface. *J. Phys. Chem. B* **2004**, *108*, 1357–1364.
- (47) García, R.; San Paulo, A. Dynamics of a vibrating tip near or in intermittent contact with a surface. *Phys. Rev. B* **2000**, *61*, No. R13381.